
Transfer Learning with Pre-trained Conditional Generative Models

Shin'ya Yamaguchi^{†‡*} Sekitoshi Kanai[†] Atsutoshi Kumagai[†]
Daiki Chijiwa[†] Hisashi Kashima[‡]
[†]NTT
[‡]Kyoto University

Abstract

Transfer learning is crucial in training deep neural networks on new target tasks. Current transfer learning methods generally assume at least one of (i) source and target task label spaces must overlap, (ii) source datasets are available, and (iii) target network architectures are consistent with source ones. However, these all assumptions are difficult to hold in practical settings because the target task rarely has the same labels as the source task, the source dataset access is restricted due to licensing and storage costs, and the target architecture is often specialized to each task. To transfer source knowledge without these assumptions, we propose a transfer learning method that uses deep generative models and is composed of the following two stages: *pseudo pre-training* (PP) and *pseudo semi-supervised learning* (P-SSL). PP trains a target architecture with a synthesized dataset by using conditional source generative models. P-SSL applies SSL algorithms to labeled target data and unlabeled pseudo samples, which are generated by cascading the source classifier and generative models to condition them with target samples. Our experimental results indicate that our method can outperform baselines of scratch training and knowledge distillation.

1 Introduction

For training deep neural networks on new tasks, *transfer learning* is essential, which leverages the knowledge of related (source) tasks to the new (target) tasks via the joint- or pre-training of source models. There are many transfer learning methods for deep models under various conditions [1, 2]. For instance, *domain adaptation* leverages source knowledge to the target task by minimizing the domain gaps [3], and *fine-tuning* uses the pre-trained weights on source tasks as the initial weights of the target models [4]. These current powerful transfer learning methods generally assume at least one of (i) source and target label spaces have overlaps, e.g., a target task composed of the same class categories as a source task, (ii) source datasets are available, and (iii) consistency of neural network architectures: the architectures in the target task must be the same as that in the source task. However, these assumptions are seldom satisfied in real-world settings. First, new target tasks do not necessarily have the label spaces overlapping with source ones because target labels are often designed on the basis of their requisites. For example, if we need to train models on StanfordCars [5], which is a fine-grained car dataset, there is no overlap with ImageNet [6] even though ImageNet has 1000 classes. Second, the accessibility of source datasets is often limited due to licensing and storage costs [7, 8, 9], e.g., ImageNet consumes over 100GB. Third, the consistency of the source and target architectures is broken if the new network architecture is specialized to the new tasks. State-of-the-art deep models are often specialized to tasks or computation resources by neural architecture search [10, 11, 12, 13]; thus, their architectures can differ for each task. Current

*Corresponding author (shinya.yamaguchi.mw@hco.ntt.co.jp)

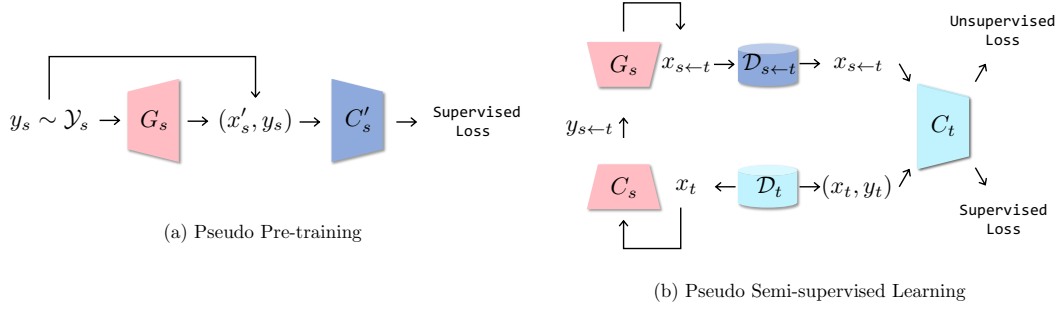


Figure 1: Proposed transfer learning methods leveraging conditional source generative model G_s . (a) We produce initial weights of target architectures through supervised task with pairs of conditional sample $x'_s \sim G_s(y_s)$ and uniformly sampled target label y_s . (b) We penalize target classifier C_t with unsupervised loss derived from SSL method by applying a pseudo sample $x_{s \leftarrow t}$ while supervised training on target dataset \mathcal{D}_t . $x_{s \leftarrow t}$ is sampled from G_s conditioned by pseudo source label $y_{s \leftarrow t} = C_s(x_t)$.

transfer learning methods are not applicable when none of the above assumptions hold, which can occur when we train a specialized target model by using the pre-trained source models in a model zoo (e.g., AWS Marketplace). Therefore, to develop deep models for the new task in such a practical setting, a new transfer learning method is required.

We shed light on an important but less studied problem setting of transfer learning, where (i) source and target task label spaces do not have overlaps, (ii) source datasets are not available, and (iii) target network architectures are not consistent with source ones. In this setting, we assume that we can access discriminative and generative models pre-trained on source datasets, the architectures of which are not the same as target models. To transfer source knowledge while satisfying the above three conditions, our main idea is to leverage the generated samples from source class-conditional generative models for training target models. From recent intensive studies [14, 15, 16], deep conditional generative models precisely replicate complex data distributions such as ImageNet, and the pre-trained models are widely available [17, 18]. By using conditional generative models, we propose a two-stage transfer learning method composed of *pseudo pre-training* (PP) and *pseudo semi-supervised learning* (P-SSL). Figure 1 illustrates an overview of our method. PP pre-trains the target architectures by using the artificial dataset assembled from the source conditional generated samples and given labels. This simple pre-process provides the effective initial weights of target models without accessing source datasets and architecture consistency. To address the non-overlap of the label spaces without accessing source datasets, P-SSL trains a target model with SSL [19, 20] by taking into account pseudo samples drawn from the conditional generative models as the unlabeled dataset. For P-SSL, pseudo samples should be target-related samples, which are samples with informative features for solving the target task. To generate target-related samples, we cascade a classifier and conditional generative model of the source domain. Specifically, we (a) obtain pseudo source soft labels from the source classifier by applying target data, and (b) generate conditional samples given a pseudo source soft label. P-SSL trains target models with current SSL algorithms by using the target-related samples as the unlabeled dataset, the distribution of which is similar enough to the target distribution.

To confirm the effectiveness of PP and P-SSL, we conducted large-scale experiments on six neural network architectures and nine vision datasets with six SSL algorithms. Our method outperformed the baselines, and the target task performance was comparable to the fine-tuning methods that require architecture consistency. This indicates that our method is practical without the architecture consistency. Furthermore, P-SSL is superior to SSL methods applied to the real target-related source datasets that are subsets of source datasets filtered by the similarity to the target dataset based on the confidence of the source classifier. This suggests that our method using pseudo soft labels can provide more meaningful information than real source samples through conditional source generative models. We also provide extensive analysis focusing on the conditions for the success of our method such as the analysis of the relationship between pseudo and target datasets.

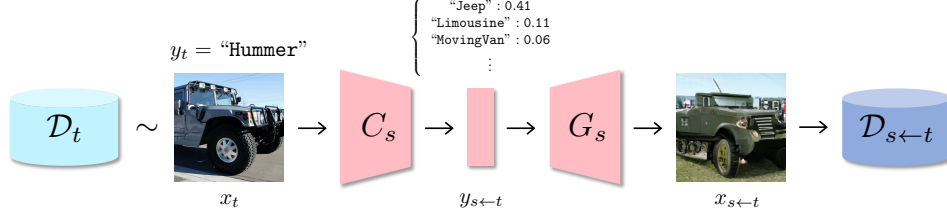


Figure 2: Pseudo conditional sampling. We obtain a pseudo soft label $y_{s \leftarrow t}$ by applying a target data x_t to a source classifier C_s , and then generate a target-related sample $x_{s \leftarrow t}$ from a source generative model G_s conditioned by $y_{s \leftarrow t}$.

2 Proposed Method

In this section, we describe our proposed method. An overview of our method is illustrated in Figure 1. PP develops initial weights for a target architecture by training with a synthesized dataset from a conditional source generative model. P-SSL takes into account the pseudo samples drawn from generative models as an unlabeled dataset in an SSL setting. In P-SSL, we generate target-related samples by *pseudo conditional sampling* (PCS, Figure 2), which cascades a source classifier and a source conditional generative model.

2.1 Problem Setting

We consider a transfer learning problem to train a deep neural network model f_θ with a trainable parameter θ on a labeled target dataset $\mathcal{D}_t = \{(x_t^i, y_t^i)\}_{i=1}^{N_t}$ without accessing a source dataset $\mathcal{D}_s = \{(x_s^i, y_s^i)\}_{i=1}^{N_s}$. Instead of source datasets, we can access a source class classifier C_s generating class probabilities by softmax function and a conditional generative model G_s (e.g., conditional GANs [21, 22]) that are pre-trained on a labeled source dataset \mathcal{D}_s . In this problem, we assume \mathcal{D}_s and \mathcal{D}_t share the input space \mathcal{X} but the label spaces \mathcal{Y}_s and \mathcal{Y}_t do not necessarily overlap. We mainly consider cases in which the target task is classification and the target model f_θ is denoted as the target classifier C_t in the below. Note that the model architectures of C_s and C_t are not necessarily the same.

2.2 Pseudo Pre-training

Without accessing source datasets and architectures consistency, we can not directly use the pre-trained weights of C_s for fine-tuning C_t . Instead of pre-training on the real source dataset, we build the useful representations of the target architecture by pre-training with a synthesized dataset from a conditional source generative model. This PP process is composed of two simple steps: (step 1) generating source conditional samples $\{G_s(y_s^i)\}_{i=1}^{N'_s}$ from uniformly sampled source labels $y_s^i \in \mathcal{Y}_s$, and (step 2) optimizing θ on the source classification task with the synthesized dataset $\mathcal{D}'_s = \{(G_s(y_s^i), y_s^i)\}_{i=1}^{N'_s}$, where N'_s is the size of the synthesized dataset by

$$\min_{\theta} \sum_{(G_s(y_s), y_s) \in \mathcal{D}'_s} \mathcal{L}_{\text{sup}}(G_s(y_s), y_s, \theta). \quad (1)$$

We use the pre-trained weights from PP as the initial weights of C_t for fine-tuning by replacing the final layer of the source task to that of the target task.

2.3 Pseudo Semi-supervised Learning

2.3.1 Semi-supervised Learning

Given a labeled dataset $\mathcal{D}_l = \{(x_l^i, y_l^i)\}_{i=1}^{N_l}$ and an unlabeled dataset $\mathcal{D}_u = \{(x_u^i)\}_{i=1}^{N_u}$, SSL is used to optimize the parameter θ of a deep neural network by solving the following problem.

$$\min_{\theta} \sum_{(x_l, y_l) \in \mathcal{D}_l} \mathcal{L}_{\text{sup}}(x_l, y_l, \theta) + \lambda \sum_{x_u \in \mathcal{D}_u} \mathcal{L}_{\text{unsup}}(x_u, \theta), \quad (2)$$

Algorithm 1 Pseudo conditional sampling

Require: Target dataset \mathcal{D}_t , source classifier C_s , source generator G_s , number of pseudo samples $N_{s \leftarrow t}$, output label function l

Ensure: Pseudo unlabeled dataset $\mathcal{D}_{s \leftarrow t}$

```
1:  $Y_{s \leftarrow t} \leftarrow \emptyset$ 
2:  $\hat{C}_s \leftarrow \text{SwapFinalLayer}(C_s, l)$ 
3: for  $x_t$  in  $\mathcal{D}_t$  do
4:    $y_{s \leftarrow t} \leftarrow \hat{C}_s(x_t)$ 
5:   Add  $y_{s \leftarrow t}$  to  $Y_{s \leftarrow t}$ 
6: end for
7: Repeat concatenating  $Y_{s \leftarrow t}$  with itself until the length reaches to  $N_{s \leftarrow t}$ 
8:  $\mathcal{D}_{s \leftarrow t} \leftarrow \emptyset$ 
9: for  $y_{s \leftarrow t}$  in  $Y_{s \leftarrow t}$  do
10:   $x_{s \leftarrow t} \sim G_s(y_{s \leftarrow t})$ 
11:  Add  $x_{s \leftarrow t}$  to  $\mathcal{D}_{s \leftarrow t}$ 
12: end for
```

where \mathcal{L}_{sup} is a supervised loss for a labeled sample (x_l, y_l) (e.g., cross-entropy loss), $\mathcal{L}_{\text{unsup}}$ is an unsupervised loss for an unlabeled sample x_u , and λ is a hyperparameter for balancing \mathcal{L}_{sup} and $\mathcal{L}_{\text{unsup}}$. In SSL, it is generally assumed that \mathcal{D}_l and \mathcal{D}_u shares the same input space \mathcal{X} .

2.3.2 Pseudo Conditional Sampling

To generate informative target-related samples, our method uses PCS, which generates target-related samples by cascading C_s and $G_s(y)$. With PCS, we first obtain a pseudo source label $y_{s \leftarrow t}$ from a source classifier C_s with a uniformly sampled x_t .

$$y_{s \leftarrow t} = C_s(x_t) \quad (3)$$

Intuitively, $y_{s \leftarrow t}$ represents the relation between source class categories and the input target sample in the form of the probabilities. We then generate target-related samples $x_{s \leftarrow t}$ with $y_{s \leftarrow t}$ as the conditional label by

$$x_{s \leftarrow t} \sim G_s(y_{s \leftarrow t}) = G_s(C_s(x_t)). \quad (4)$$

Although it is generally assumed with conditional generative models that discrete (one-hot) class labels are the input and the trained models can generate class-wise interpolated samples by the continuously mixed labels of multiple class categories [22, 23]. By leveraging this characteristic, we aim to generate target-related samples by $y_{s \leftarrow t}$ constructed with an interpolation of source classes.

For the training of the target task, we compose a pseudo dataset $\mathcal{D}_{s \leftarrow t}$ by applying Algorithm 1. In line 2, we swap the final layer of C_s (in general, a softmax function) with an output label function l , which determines the form of output of C_s . For example, we can choose $\arg \max$ or the temperature softmax function as l instead of a softmax function. We empirically found that a softmax function is the best choice for l through the comparison results presented in Sec. C.3.2

2.3.3 Training

Since we use x_t to generate $x_{s \leftarrow t}$, one can assign the label y_t of x_t . However, it is difficult to directly use $(x_{s \leftarrow t}, y_t)$ in supervised learning because $x_{s \leftarrow t}$ does not necessarily preserve the target label information; we empirically confirm that this naïve approach fails to boost the target performance mentioned in Sec. 3.8.1. To extract informative knowledge from $x_{s \leftarrow t}$, we propose P-SSL, which trains a target classifier C_t in the fashion of SSL by using a labeled target dataset \mathcal{D}_t and an unlabeled dataset $\mathcal{D}_{s \leftarrow t}$ generated by PCS. Our idea is to exploit the self-training assumption of SSL [19, 24]: the high-confidence prediction of training models for unlabeled data tend to be correct. That is, we use the prediction $C_t(x_{s \leftarrow t})$ as the soft label of $x_{s \leftarrow t}$ for training C_t . In the training, C_t interprets $x_{s \leftarrow t}$ as the mixture of target classes rather than forces to classify it into one class. This can make models learn the information interpolating the target classes and acquire the high prediction accuracy toward unseen samples. Borrowing unlabeled loss functions of SSL, we compute the unsupervised loss function for a pseudo sample $x_{s \leftarrow t}$ as $\mathcal{L}_{\text{unsup}}(x_{s \leftarrow t}, \theta)$. We can adopt arbitrary SSL algorithms

Table 1: List of target datasets. We constructed Caltech-256-60 by randomly sampled 60 images per class from the original dataset in accordance with procedure of [27].

Dataset	Task	Classes	Size (Train/Test)
Caltech-256-60	General Object Recognition	256	15,360/15,189
CUB-200-2011	Finegrained Object Recognition	200	5,994/5,794
DTD	Texture Recognition	47	3,760/1,880
FGVC-Aircraft	Finegrained Object Recognition	100	6,667/3,333
Indoor67	Scene Recognition	67	5,360/1,340
OxfordFlower	Finegrained Object Recognition	102	2,040/6,149
OxfordPets	Finegrained Object Recognition	37	3,680/3,369
StanfordCars	Finegrained Object Recognition	196	8,144/8,041
StanfordDogs	Finegrained Object Recognition	120	12,000/8,580

using soft labels for calculating $\mathcal{L}_{\text{unsup}}$; we compare SSL algorithms in Sec. 3.8.1. For instance, $\mathcal{L}_{\text{unsup}}$ using UDA [25] is

$$\mathbb{1} \left(\max_{y' \in \hat{C}_t(x, \tau)} y' > \beta \right) \text{CE} \left(\hat{C}_t(x, \tau), C_t(T(x)) \right), \quad (5)$$

where $\mathbb{1}$ is an indicator function, CE is a cross entropy function, $\hat{C}_t(x, \tau)$ is the target classifier replacing the final layer with the temperature softmax function with a temperature hyperparameter τ , β is a confidence threshold, and $T(\cdot)$ is an input transformation function such as RandAugment [26]. Eventually, we optimize the parameter θ of C_t with the pre-trained models C_s and G_s on the basis of the objective function of SSL in Eq (2) as

$$\min_{\theta} \sum_{x_t, y_t \in \mathcal{D}_t} \mathcal{L}_{\text{sup}}(x_t, y_t, \theta) + \lambda \sum_{x_{s \leftarrow t} \in \mathcal{D}_{s \leftarrow t}} \mathcal{L}_{\text{unsup}}(x_{s \leftarrow t}, \theta). \quad (6)$$

In this method, since we treat $x_{s \leftarrow t} \sim G_s(C_s(x_t))$ as the unlabeled sample of the target task, the following assumption is required.

Assumption 2.1. $p_t(x) \approx \frac{1}{|D_t|} \sum_{x_t} p_{G_s(C_s(x_t))}(x)$,

where $p_t(x)$ is a target data distribution. That is, if pseudo samples satisfy Assumption 2.1, P-SSL should boost the target task performance by P-SSL. We empirically discuss the detailed conditions of P-SSL in Sec. 3.8.2 through evaluating the distance between the target distribution and the distributions of pseudo samples.

3 Experiments

We evaluate our method with multiple target architectures and datasets and compare it with baselines including scratch training and knowledge distillation that can be applied to our problem setting with simple modification. We further conduct detailed analyses of our pseudo pre-training (PP) and pseudo semi-supervised learning (P-SSL) in terms of (i) the comparison of our methods and the methods accessing real source datasets, (ii) performance studies with lower volume target datasets, (iii) analysis including the variation studies of the synthesized datasets for PP, (iv) analysis including ablations of SSL algorithms and distribution gaps between target and pseudo datasets for P-SSL.

3.1 Setting

3.1.1 Baselines

We evaluated our method by comparing it with the scratch training method (**Scratch**), which trains a model with only a target dataset, and naïve knowledge distillation methods **Logit Matching** [28] and **Soft Target** [29]. Logit Matching and Soft Target can be used for transfer learning under architecture inconsistency since their loss functions use only final logit outputs of models regardless of the intermediate layers. To transfer knowledge in C_s to C_t , we first fine-tune the parameters of C_s on the target task, and then train C_t with knowledge distillation penalties by treating the trained C_s -based model as the teacher model. We provide more details in Appendix B.1.

Table 2: Performance comparison of multiple target architectures on StanfordCars (Top-1 Acc.(%))

	ResNet-50	WRN-50-2	MNASNet1.0	MobileNetV3-L	EfficientNet-B0	EfficientNet-B5
Scratch	76.21 \pm 1.40	76.92 \pm 2.16	81.08 \pm 0.06	82.67 \pm 0.21	82.50 \pm 0.47	85.09 \pm 1.01
Logit Matching	84.36 \pm 0.47	86.28 \pm 1.13	85.08 \pm 0.08	86.00 \pm 0.28	86.37 \pm 0.69	88.42 \pm 0.60
Soft Target	79.95 \pm 1.62	82.34 \pm 1.15	83.55 \pm 1.21	84.64 \pm 0.21	85.16 \pm 0.69	85.30 \pm 1.37
Pseudo Pre-training (PP)	90.25 \pm 0.19	90.95 \pm 0.21	87.14 \pm 0.05	88.19 \pm 0.14	88.27 \pm 0.33	89.50 \pm 0.17
P-UDA	80.14 \pm 0.57	78.90 \pm 0.82	82.22 \pm 0.16	83.26 \pm 0.21	83.22 \pm 0.54	85.82 \pm 0.47
PP + P-UDA	90.69\pm0.11	91.76\pm0.41	87.39\pm0.19	88.40\pm0.67	89.28\pm0.41	90.04\pm0.34

Table 3: Performance comparison of ResNet-50 classifiers on multiple target datasets (Top-1 Acc. (%))

	Caltech-256-60	CUB-200-2011	DTD	FGVC-Aircraft	Indoor67	OxfordFlower	OxfordPets	StanfordCars	StanfordDogs
Scratch	51.03 \pm 1.10	52.98 \pm 1.14	42.58 \pm 2.57	72.02 \pm 4.16	49.70 \pm 1.67	68.57 \pm 1.79	63.31 \pm 1.20	76.21 \pm 1.40	57.46 \pm 1.70
Logit Matching	55.22 \pm 1.25	64.10 \pm 0.85	39.49 \pm 1.67	78.87 \pm 2.05	56.12 \pm 1.16	69.03 \pm 1.25	70.69 \pm 1.11	84.36 \pm 0.47	66.22 \pm 1.36
Soft Target	53.65 \pm 0.39	57.86 \pm 0.85	41.17 \pm 2.52	77.26 \pm 0.62	50.92 \pm 0.91	66.51 \pm 3.02	62.93 \pm 3.75	79.95 \pm 1.62	58.71 \pm 3.71
Pseudo Pre-training (PP)	68.69 \pm 0.08	75.73 \pm 0.33	55.53 \pm 1.07	86.02 \pm 0.40	65.60 \pm 0.62	93.80\pm0.61	86.57 \pm 0.37	90.25 \pm 0.19	72.80 \pm 0.15
P-UDA	53.12 \pm 0.99	54.81 \pm 0.26	38.71 \pm 3.11	72.59 \pm 0.05	50.60 \pm 1.86	69.41 \pm 2.41	64.51 \pm 0.48	80.14 \pm 0.57	60.66 \pm 1.36
PP + P-UDA	70.02\pm0.62	76.01\pm0.58	56.35\pm1.07	86.54\pm0.31	66.84\pm0.15	90.35 \pm 0.12	87.85\pm0.59	90.69\pm0.11	73.56\pm0.25

3.1.2 Datasets

We used ImageNet [6] as the default source datasets. In Sec. 3.5, we report the case of applying CompCars [30] as the source dataset. For target datasets, we used the nine classification datasets listed in Table 1 for the evaluation discussed in Sec. 3.3. We used these datasets with the intent to include various granularities and domains. Note that StanfordDogs is a subset of ImageNet, thus has the overlap of the label space to ImageNet, but we added this dataset to confirm the performance when the overlapping exist. In the other experiments, we used StanfordCars [5], which is for a fine-grained classification of car types, as the target dataset.

3.1.3 Network Architecture

As a source classifier C_s , we used the ResNet-50 architecture [31] with the pre-trained weight distributed by torchvision official repository.² For a target classifier C_t , we used six architectures: ResNet-50 [31], WRN-50-2 [32], MNASNet1.0 [33], MobileNetV3-L [34], and EfficientNet-B0/B5 [11]; we implemented them and applied the pre-trained weights provided in torchvision. For a source conditional generative model G_s , we used BigGAN [14] generating 256×256 resolution images as the default architecture. We also tested the other generative models such as ADM-G [16] in Sec. C.2. We implemented BigGAN on the basis of open source repositories including pytorch-pretrained-BigGAN³; we used the pre-trained weights distributed by the repositories.

3.1.4 Training

We selected the training configurations on the basis of the previous works [35, 25]. In PP, we trained a source classifier by Neterov momentum SGD for 100 epochs with a mini-batch size of 128, weight decay of 0.0001, momentum of 0.9, and initial learning rate of 0.1; we decayed the learning rate by 0.1 at 30, 60, 90 epochs. We used the 1.3M generated images by the ImageNet pre-trained BigGAN (256×256 resolution). We trained a target classifier C_t by Neterov momentum SGD for 300 epochs with a mini-batch size of 16, weight decay of 0.0001, and momentum of 0.9. We set the initial learning rate to 0.05 for the scratch models and 0.005 for the models with PP. We dropped the learning rate by 0.1 at 150 and 250 epochs. For each target dataset, we split the training set into 9 : 1, and used the former in the training and the later in validating. The input samples were resized into 224×224 resolution. For the SSL algorithms, we set the mini-batch size for $\mathcal{L}_{\text{unsup}}$ to 112, and fixed λ in Eq. (2) to 1. We used UDA [25] as the default SSL algorithm because it achieves the best result; we compare and discuss applying the other SSL algorithms in Sec. 3.8.1. We fixed the hyperparameters of UDA as the confidence threshold $\beta = 0.5$ and the temperature parameter $\tau = 0.4$ following [25]. We denote the models trained in P-SSL (hereafter, P-SSL models) by applying UDA as **P-UDA** in the below. For P-UDA, we generated 50,000 samples by PCS. We ran the target trainings three times with different seeds and selected the best models in terms of the validation accuracy for each epoch. We report the average top-1 test accuracies and standard deviations.

²<https://github.com/pytorch/vision>

³<https://github.com/huggingface/pytorch-pretrained-BigGAN>

Table 4: Comparison to fine-tuning (FT) and semi-supervised learning (SSL) on StanfordCars

Generative Model	Top-1 Acc. (%)		FID($\mathcal{D}_{s \leftarrow t}, \mathcal{D}_t$)
	PP	P-UDA	
BigGAN [23]	90.25 \pm 0.19	80.14 \pm 0.57	19.92
Real Dataset	FT	R-UDA	FID($\mathcal{D}_s, \mathcal{D}_t$)
All ImageNet	90.56 \pm 0.17	75.28 \pm 2.97	147.27
Filtered ImageNet	73.18 \pm 2.77	77.48 \pm 0.46	54.76

Table 5: Comparison of source datasets on StanfordCars

	Source Dataset	
	ImageNet	CompCars
Pseudo Pre-training (PP)	90.25 \pm 0.19	86.57 \pm 0.37
P-UDA	80.14 \pm 0.57	79.12 \pm 0.25
PP + P-UDA	90.69 \pm 0.11	86.80 \pm 0.26

3.2 Target Architecture

We first discuss the performance evaluations by varying the neural network architectures of the target classifiers. Table 2 lists the results on StanfordCars with multiple target architectures. Note that we evaluated our method by fixing the source architecture to ResNet-50. P-UDA outperformed the baselines on all target architectures. This indicates that our method boosts target models without any architecture consistency between source and target tasks.

3.3 Target Datasets

We show the efficacy of our method on multiple target datasets. We used ResNet-50 as the architecture of the target classifiers. Although the target and source architectures were same, we did not use the pre-trained weights of the source models when training C_t . Table 3 lists the top-1 accuracy of each classification task. The Scratch row are the results of using the target datasets only. PP significantly outperformed the baselines on all target datasets. This suggests that building basic representation by pre-training is effective for various target tasks even if the source dataset is drawn from generative models. For P-UDA, we observed that it boosted the scratch models in all target datasets except for DTD and OxfordFlower, and the combination of PP and P-UDA achieved the best performance. As the reasons for the degradation, we consider that the pseudo samples do not satisfy Assumption 2.1. We explore this by considering the relationship between pseudo and target distributions in Sec. 3.8.2.

3.4 Comparison to Methods with Real Source Dataset

To confirm the practicality of our method, we compared it with methods accessing real source datasets. We tested **Fine-tuning (FT)** and **R-UDA**, which use a real source dataset for the pre-training and the semi-supervised learning of UDA. We measured the top-1 test accuracy on StanfordCars and also Fréchet Inception Distance (FID, [36]), which is a metric for evaluating generative models (lower value is better). For FT and R-UDA, we used ImageNet and a subset of ImageNet (Filtered ImageNet), which was collected by confidence-based filtering similar to a previous study [25]. We provide more details in Appendix B.2. In Table 4, the PP model was competitive with FT. This suggests that the synthesized dataset used in PP can near-perfectly preserve essential information of the original source dataset for pre-training target architectures, i.e., real source datasets may not be necessary for pre-training. On the other hand, P-UDA was superior to R-UDA on top-1 accuracy. By comparing FID($\mathcal{D}_{s \leftarrow t}, \mathcal{D}_t$) and FID($\mathcal{D}_s, \mathcal{D}_t$), we can confirm that the fidelity of the pseudo samples toward the real target samples is significantly better than the real samples. This means that the generated samples by PCS can contain more useful information for SSL than real target-related samples.

3.5 Source Datasets

We investigate the preferable characteristics of source datasets for PP and P-SSL by testing another source dataset, which was CompCars [30], a fine-grained vehicle dataset containing 136K images (see Appendix B.3 for details). This is more similar to the target dataset (StanfordCars) than ImageNet. All training settings were the same as mentioned in Sec. 3.1. We constructed the source task as the classification task predicting 163 classes of car manufacturers. Table 5 lists the scores for each model of our methods. The models using ImageNet were superior to those using CompCars. To seek the difference, we measured FID($\mathcal{D}_{s \leftarrow t}, \mathcal{D}_t$) when using CompCars as with the protocol in Sec. 3.4, and the score was 22.12, which is inferior to the score when using ImageNet (19.92). This suggests that the fidelity of pseudo samples toward target samples is important to boost the target performance and is not simply determined by the similarity between the source and target datasets. We consider that

Table 6: Top-1 accuracy in various target dataset sizes

	Sampling Rate		
	25%	50%	75%
Scratch	5.05 \pm 0.67	37.34 \pm 4.91	65.38 \pm 3.93
Logit Matching	11.04 \pm 2.04	63.61 \pm 2.50	78.29 \pm 1.32
Soft Target	5.48 \pm 0.61	54.87 \pm 3.52	68.40 \pm 1.24
Pseudo Pre-training (PP)	59.96 \pm 0.13	81.99 \pm 0.11	87.76 \pm 0.05
P-UDA	7.20 \pm 0.52	42.29 \pm 1.12	67.29 \pm 0.88
PP + P-UDA	61.79\pm0.14	82.21\pm0.43	88.27\pm0.21

Table 7: Comparison of pseudo pre-training variants

	Top-1 Acc. (%)
Uniform	90.25\pm0.19
Filtered	84.89 \pm 0.23
PCS	85.90 \pm 0.35

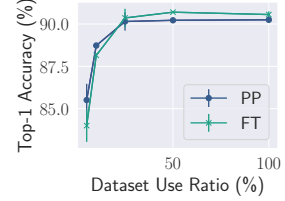


Figure 3: Scaling synthesized dataset size

the diversity of source classes provides the usefulness of pseudo samples; thus ImageNet is superior to CompCars as the source dataset.

3.6 Target Dataset Size

We evaluate the performance of our method on a limited target data setting. We randomly sampled the subsets of the training dataset (StanfordCars) for each sampling rate of 25, 50, and 75%, and used them to train target models with our method. Note that the pseudo datasets were created by using the reduced datasets. Table 6 lists the results. We observed that our method can outperform the baselines in all sampling rate settings.

3.7 Analysis of Pseudo Pre-training

We analyze the characteristics of PP by varying the synthesized datasets.

3.7.1 Synthesizing Strategy

We first compare the three strategies using the source generative models for PP. We tested **Uniform**: synthesizing samples for all source classes (default), **Filtered**: synthesizing samples for target-related source classes identified by the same protocol as in Sec. 3.4, **PCS**: synthesizing samples by PCS. In PCS, we optimized the pre-training models with pseudo source soft labels generated in the process of PCS. Table 7 shows the target task performances. We found that the Uniform model achieved the best performance. We can infer that, in PP, pre-training with various classes is more important than that with only target-related classes, in contrast to P-SSL.

3.7.2 Synthesized Dataset Size

Next, we evaluate PP by scaling the synthesized dataset size. Figure 3 illustrates the transitions of the target top-1 accuracy on the dataset size. We denote the dataset size as a ratio when the case of 1.3M images is 100%. We also show the results of FT with real ImageNet. PP gradually degraded its performance in accordance with the dataset size reduction, but achieved near equivalent performance to that of FT. This indicates that the synthesized datasets can preserve commensurate information as the real datasets; thus, we can compress the information into generative models, which is much smaller than source datasets.

3.8 Analysis of Pseudo Semi-supervised Learning

3.8.1 Semi-supervised Learning Algorithm

We compare SSL algorithms in P-SSL. We used six SSL algorithms: EntMin [37], Pseudo Label [38], Soft Pseudo Label, Consistency Regularization, FixMatch [39], and UDA [25]. Soft Pseudo Label is a variant of Pseudo Label, which uses the sharpen soft pseudo labels instead of the one-hot (hard) pseudo labels. Consistency Regularization computes the unsupervised loss of UDA without the confidence thresholding. Table 8 shows the results on StanfordCars, where Pseudo Supervised is a model using a pairs of $(x_{s \leftarrow t}, y_t)$ in pseudo conditional sampling for supervised training. UDA achieved the best result. More importantly, the methods using hard labels (Pseudo Supervised, Pseudo Label, and FixMatch) failed to outperform the scratch models, whereas the soft label based methods improved the performance. This indicates that translating the label of pseudo samples as the interpolation of the target labels can improve the performance as mentioned in Sec. 2.3.3.

Table 8: Comparison of algorithms for P-SSL

	Top-1 Acc. (%)
Scratch	76.21 \pm 1.40
Pseudo Supervised	53.03 \pm 1.79
EntMin [37]	72.56 \pm 3.33
Pseudo Label [38]	74.49 \pm 2.26
Soft Pseudo Label	78.44 \pm 2.41
Consistency Regularization	79.17 \pm 1.79
FixMatch [39]	74.31 \pm 3.27
UDA [25]	80.14 \pm 0.57

Table 9: FID and target test accuracy on multiple target datasets

	Top-1 Acc. (%)			FID		
	Scratch	P-UDA	Diff.	$(\mathcal{D}_s, \mathcal{D}_t)$	$(F(\mathcal{D}_s), \mathcal{D}_t)$	$(\mathcal{D}_{s \leftarrow t}, \mathcal{D}_t)$
Caltech-256-60	51.03	53.12	+2.09	31.27	87.18	19.69
CUB-200-2011	52.98	54.81	+1.83	131.85	65.34	19.15
DTD	42.85	38.71	-4.15	100.51	82.63	87.57
FGVC-Aircraft	72.07	72.59	+0.53	189.16	47.29	23.68
Indoor67	49.70	50.60	+0.90	96.68	44.09	34.27
OxfordFlower102	68.57	69.41	+0.84	190.33	137.64	118.39
OxfordPets	63.31	64.51	+1.21	95.16	20.59	16.94
StanfordCars	76.21	80.14	+3.93	147.27	54.76	19.92
StanfordDogs	57.46	60.66	+3.20	80.94	6.09	7.34

3.8.2 Relationship between Datasets

As discussed in Sec. 2.3, P-SSL requires the assumption of that the distribution of the pseudo samples approximates the target data distribution. In this section, we empirically explore the condition for the success of P-SSL in terms of the relationships between datasets. We used FID, which is also used in Sec. 3.4. We measured the FID among a target dataset \mathcal{D}_t , source dataset \mathcal{D}_s , filtered source dataset $F(\mathcal{D}_s)$, and pseudo dataset $\mathcal{D}_{s \leftarrow t}$. We constructed $F(\mathcal{D}_s)$ for each target dataset by using the same protocol described in Sec. 3.4. Table 9 shows the FID scores and the top-1 accuracies on multiple target datasets. We observe that $\text{FID}(F(\mathcal{D}_s), \mathcal{D}_t)$ are more correlated to accuracy (correlation coefficient $r = 0.32$) than $\text{FID}(\mathcal{D}_s, \mathcal{D}_t)$ ($r = 0.04$), indicating that the similarity between a target dataset and target-related subset of source datasets is more important than that of a whole source dataset. We also found that $\text{FID}(\mathcal{D}_{s \leftarrow t}, \mathcal{D}_t)$ is better than $\text{FID}(F(\mathcal{D}_s), \mathcal{D}_t)$ in most cases and is the best indicator for accuracy prediction ($r = 0.61$). This indicates that the pseudo dataset by PCS can produce more target-related information than real datasets, and that the quality of the pseudo samples compared with that of the target samples is crucial for achieving better target performance. We further explored the effects of $\text{FID}(\mathcal{D}_{s \leftarrow t}, \mathcal{D}_t)$ on a single target dataset (StanfordCars) with multiple generative models (see Appendix C.2 and C.3.2). In Figure 4, we plot the relationship $\text{FID}(\mathcal{D}_{s \leftarrow t}, \mathcal{D}_t)$ and top-1 target test accuracy. As with Table 9, we can confirm that the better FID score improves the target performance. From the above observations, we conclude that the key factors of P-SSL are (a) the similarity of target datasets and target-related subsets of source datasets and (b) the capability of source generative models for generating high-quality target-related samples.

4 Related Work

4.1 Deep Inductive Transfer Learning

Our method is categorized as an inductive transfer learning approach [1], where labeled target datasets are available and source and target task label spaces have no overlapping. In deep learning, fine-tuning [4, 40, 41], which leverages source pre-trained weights as initial parameters of target models, is one of the most common inductive transfer learning approaches because of its simplicity. We describe several fine-tuning methods in Appendix A. In contrast, our method can be used without consistency of model architectures and source dataset access since it transfers source knowledge via pseudo samples drawn from source pre-trained generative models. In Sec. 3 and Appendix C, we show that the target performance of our method is closed to that of fine-tuning methods.

4.2 Semi-supervised Learning

SSL is a paradigm that trains a supervised model with labeled and unlabeled samples by minimizing supervised and unsupervised loss simultaneously. Historically, various SSL algorithms have been used or proposed for deep learning such as entropy minimization [37], pseudo-label [38], virtual adversarial training [42], and consistency regularization [43, 44, 45]. UDA [25] and FixMatch [39], which combine ideas of pseudo-label and consistency regularization, have achieved remarkable performance. An assumption with these SSL algorithms is that the unlabeled data are sampled from the same distribution as the labeled data. If there is a large gap between the labeled and unlabeled data distribution, the performance of SSL algorithms degrades [46]. However, Xie et al. [25] have empirically revealed that unlabeled samples in another dataset different from a target dataset can improve the performance of SSL algorithms by carefully selecting target-related samples from source

datasets. This indicates that SSL algorithms can achieve high performances as long as the unlabeled samples are related to target datasets, even when they belong to different datasets. On the basis of this implication, P-SSL with our method exploits pseudo source samples drawn from generative models as unlabeled data for SSL. We tested SSL algorithms for P-SSL and compared the resulting P-SSL models with SSL models using the filtered real source dataset constructed by the protocol of [25].

4.3 Training Techniques Applying Generative Models

Similar to our study, several studies have applied the expressive power of conditional generative models to boost the performance of discriminative models (e.g., classifiers); Zhu et al. [47] and Yamaguchi et al. [48] have exploited the generated images from conditional GANs for data augmentation in classification, and Sankaranarayanan et al. [49] have introduced conditional GANs into the system of domain adaptation for learning joint-feature spaces of source and target domains. Moreover, Li et al. [50] have implemented an unsupervised domain adaptation technique with conditional GANs in a setting of no accessing source datasets. These studies require label overlapping between source and target tasks or training of generative models on target datasets, which causes problems of overfitting and mode collapse when the target datasets are small [51, 52, 15]. Our method, however, requires no additional training of generative models because it simply extracts samples from fixed pre-trained conditional generative models.

5 Conclusion

We proposed a transfer learning method leveraging pre-trained conditional source generative models, which is composed of PP and P-SSL. PP builds useful representations on a target architecture and P-SSL applies an SSL algorithm by taking into account the pseudo samples from the generative models as the unlabeled dataset. Our experiments showed that our method is superior to baselines and is competitive with fine-tuning. An important future step is to modify pre-training by using self-supervised learning that trains a model without class labels and conditioning the generative models by applying information retrieval methods.

References

- [1] S. J. Pan and Q. Yang. A survey on transfer learning. *IEEE Transactions on Knowledge and Data Engineering*, 22(10), Oct 2010.
- [2] Mei Wang and Weihong Deng. Deep visual domain adaptation: A survey. *Neurocomputing*, 2018.
- [3] Yaroslav Ganin, Evgeniya Ustinova, Hana Ajakan, Pascal Germain, Hugo Larochelle, François Laviolette, Mario Marchand, and Victor Lempitsky. Domain-adversarial training of neural networks. *The journal of machine learning research*, 2016.
- [4] Jason Yosinski, Jeff Clune, Yoshua Bengio, and Hod Lipson. How transferable are features in deep neural networks? In *Advances in Neural Information Processing Systems*, 2014.
- [5] Jonathan Krause, Michael Stark, Jia Deng, and Li Fei-Fei. 3d object representations for fine-grained categorization. In *4th International IEEE Workshop on 3D Representation and Recognition*, Sydney, Australia, 2013.
- [6] Olga Russakovsky, Jia Deng, Hao Su, Jonathan Krause, Sanjeev Satheesh, Sean Ma, Zhiheng Huang, Andrej Karpathy, Aditya Khosla, Michael Bernstein, et al. Imagenet large scale visual recognition challenge. *International Journal of Computer Vision*, 115(3), 2015.
- [7] Jian Liang, Dapeng Hu, and Jiashi Feng. Do we really need to access the source data? Source hypothesis transfer for unsupervised domain adaptation. In *Proceedings of the 37th International Conference on Machine Learning*, 2020.
- [8] Jogendra Nath Kundu, Naveen Venkat, Rahul M V, and R. Venkatesh Babu. Universal source-free domain adaptation. In *Proceedings of the IEEE/CVF Conference on Computer Vision and Pattern Recognition*, 2020.
- [9] Dequan Wang, Evan Shelhamer, Shaoteng Liu, Bruno Olshausen, and Trevor Darrell. Tent: Fully test-time adaptation by entropy minimization. In *International Conference on Learning Representations*, 2021.
- [10] Barret Zoph and Quoc V Le. Neural architecture search with reinforcement learning. In *International Conference on Learning Representation*, 2017.
- [11] Mingxing Tan and Quoc Le. EfficientNet: Rethinking model scaling for convolutional neural networks. In *International Conference on Machine Learning*, 2019.
- [12] Dilin Wang, Chengyue Gong, Meng Li, Qiang Liu, and Vikas Chandra. Alphanet: Improved training of supernets with alpha-divergence. In *International Conference on Machine Learning*, 2021.
- [13] Hayeon Lee, Eunyoung Hyung, and Sung Ju Hwang. Rapid neural architecture search by learning to generate graphs from datasets. In *International Conference on Learning Representations*, 2021.
- [14] Andrew Brock, Jeff Donahue, and Karen Simonyan. Large scale gan training for high fidelity natural image synthesis. In *International Conference on Learning Representations*, 2018.
- [15] Tero Karras, Miika Aittala, Janne Hellsten, Samuli Laine, Jaakko Lehtinen, and Timo Aila. Training generative adversarial networks with limited data. In *Advances in Neural Information Processing Systems*, 2020.
- [16] Prafulla Dhariwal and Alex Nichol. Diffusion models beat gans on image synthesis. In *Advances in Neural Information Processing Systems*, 2021.
- [17] Yaxing Wang, Chenshen Wu, Luis Herranz, Joost van de Weijer, Abel Gonzalez-Garcia, and Bogdan Raducanu. Transferring gans: generating images from limited data. In *Proceedings of the European Conference on Computer Vision*, 2018.
- [18] Miaoyun Zhao, Yulai Cong, and Lawrence Carin. On leveraging pretrained gans for generation with limited data. In *International Conference on Machine Learning*, pages 11340–11351. PMLR, 2020.
- [19] Olivier Chapelle, Bernhard Schölkopf, and Alexander Zien. *Semi-supervised Learning*. MIT Press, 2006.
- [20] Jesper E Van Engelen and Holger H Hoos. A survey on semi-supervised learning. *Machine Learning*, 2020.

- [21] Augustus Odena, Christopher Olah, and Jonathon Shlens. Conditional image synthesis with auxiliary classifier gans. In *International Conference on Machine Learning*, 2017.
- [22] Takeru Miyato and Masanori Koyama. cGANs with projection discriminator. *International Conference on Learning Representations*, 2018.
- [23] Andrew Brock, Jeff Donahue, and Karen Simonyan. Large scale GAN training for high fidelity natural image synthesis. In *International Conference on Learning Representations*, 2019.
- [24] Xiangli Yang, Zixing Song, Irwin King, and Zenglin Xu. A survey on deep semi-supervised learning. *arXiv preprint arXiv:2103.00550*, 2021.
- [25] Qizhe Xie, Zihang Dai, Eduard Hovy, Thang Luong, and Quoc Le. Unsupervised data augmentation for consistency training. In *Advances in Neural Information Processing Systems*, 2020.
- [26] Ekin D Cubuk, Barret Zoph, Jonathon Shlens, and Quoc V Le. Randaugment: Practical automated data augmentation with a reduced search space. In *Proceedings of the IEEE/CVF Conference on Computer Vision and Pattern Recognition Workshops*, pages 702–703, 2020.
- [27] Yin Cui, Yang Song, Chen Sun, Andrew Howard, and Serge Belongie. Large scale fine-grained categorization and domain-specific transfer learning. In *Proceedings of the IEEE conference on computer vision and pattern recognition*, 2018.
- [28] Jimmy Ba and Rich Caruana. Do deep nets really need to be deep? In *Advances in Neural Information Processing Systems*, 2014.
- [29] Geoffrey Hinton, Oriol Vinyals, and Jeff Dean. Distilling the knowledge in a neural network. *arXiv preprint arXiv:1503.02531*, 2015.
- [30] Linjie Yang, Ping Luo, Chen Change Loy, and Xiaoou Tang. A large-scale car dataset for fine-grained categorization and verification. In *Proceedings of the IEEE conference on computer vision and pattern recognition*, 2015.
- [31] Kaiming He, Xiangyu Zhang, Shaoqing Ren, and Jian Sun. Deep residual learning for image recognition. In *Proceedings of the IEEE conference on computer vision and pattern recognition*, 2016.
- [32] Sergey Zagoruyko and Nikos Komodakis. Wide residual networks. In *British Machine Vision Conference 2016*, 2016.
- [33] Mingxing Tan, Bo Chen, Ruoming Pang, Vijay Vasudevan, Mark Sandler, Andrew Howard, and Quoc V Le. Mnasnet: Platform-aware neural architecture search for mobile. In *Proceedings of the IEEE/CVF Conference on Computer Vision and Pattern Recognition*, 2019.
- [34] Andrew Howard, Mark Sandler, Grace Chu, Liang-Chieh Chen, Bo Chen, Mingxing Tan, Weijun Wang, Yukun Zhu, Ruoming Pang, Vijay Vasudevan, et al. Searching for mobilenetv3. In *Proceedings of the IEEE/CVF International Conference on Computer Vision*, pages 1314–1324, 2019.
- [35] Hao Li, Pratik Chaudhari, Hao Yang, Michael Lam, Avinash Ravichandran, Rahul Bhotika, and Stefano Soatto. Rethinking the hyperparameters for fine-tuning. In *International Conference on Learning Representations*, 2020.
- [36] Martin Heusel, Hubert Ramsauer, Thomas Unterthiner, Bernhard Nessler, and Sepp Hochreiter. Gans trained by a two time-scale update rule converge to a local nash equilibrium. In *Advances in Neural Information Processing Systems*, 2017.
- [37] Yves Grandvalet and Yoshua Bengio. Semi-supervised learning by entropy minimization. In *Advances in Neural Information Processing Systems*, 2005.
- [38] Dong-Hyun Lee et al. Pseudo-label: The simple and efficient semi-supervised learning method for deep neural networks. In *Workshop on challenges in representation learning, ICML*, 2013.
- [39] Kihyuk Sohn, David Berthelot, Nicholas Carlini, Zizhao Zhang, Han Zhang, Colin A Raffel, Ekin Dogus Cubuk, Alexey Kurakin, and Chun-Liang Li. Fixmatch: Simplifying semi-supervised learning with consistency and confidence. In *Advances in Neural Information Processing Systems*, 2020.
- [40] Pulkit Agrawal, Ross Girshick, and Jitendra Malik. Analyzing the performance of multilayer neural networks for object recognition. In *European conference on computer vision*, 2014.

- [41] Ross Girshick, Jeff Donahue, Trevor Darrell, and Jitendra Malik. Rich feature hierarchies for accurate object detection and semantic segmentation. In *Proceedings of the IEEE conference on computer vision and pattern recognition*, 2014.
- [42] Takeru Miyato, Shin-ichi Maeda, Masanori Koyama, and Shin Ishii. Virtual adversarial training: a regularization method for supervised and semi-supervised learning. *IEEE transactions on pattern analysis and machine intelligence*, 2017.
- [43] Philip Bachman, Ouais Alsharif, and Doina Precup. Learning with pseudo-ensembles. In *Advances in neural information processing systems*, 2014.
- [44] Mehdi Sajjadi, Mehran Javanmardi, and Tolga Tasdizen. Regularization with stochastic transformations and perturbations for deep semi-supervised learning. In *Advances in neural information processing systems*, 2016.
- [45] Samuli Laine and Timo Aila. Temporal ensembling for semi-supervised learning. In *International Conference on Learning Representations*, 2016.
- [46] Avital Oliver, Augustus Odena, Colin Raffel, Ekin Dogus Cubuk, and Ian Goodfellow. Realistic evaluation of semi-supervised learning algorithms. In *Advances in Neural Information Processing Systems*, 2018.
- [47] Yezi Zhu, Marc Aoun, Marcel Krijn, and Joaquin Vanschoren. Data augmentation using conditional generative adversarial networks for leaf counting in arabidopsis plants. In *British Machine Vision Conference*, 2018.
- [48] Shin'ya Yamaguchi, Sekitoshi Kanai, and Takeharu Eda. Effective data augmentation with multi-domain learning gans. In *Proceedings of the AAAI Conference on Artificial Intelligence*, 2020.
- [49] Swami Sankaranarayanan, Yogesh Balaji, Carlos D Castillo, and Rama Chellappa. Generate to adapt: Aligning domains using generative adversarial networks. In *Proceedings of the IEEE Conference on Computer Vision and Pattern Recognition*, 2018.
- [50] Rui Li, Qianfen Jiao, Wenming Cao, Hau-San Wong, and Si Wu. Model adaptation: Unsupervised domain adaptation without source data. In *Proceedings of the IEEE/CVF Conference on Computer Vision and Pattern Recognition*, 2020.
- [51] Han Zhang, Zizhao Zhang, Augustus Odena, and Honglak Lee. Consistency regularization for generative adversarial networks. In *International Conference on Learning Representations*, 2020.
- [52] Shengyu Zhao, Zhijian Liu, Ji Lin, Jun-Yan Zhu, and Song Han. Differentiable augmentation for data-efficient gan training. In *Advances in neural information processing systems*, 2020.
- [53] Boris Chidlovskii, Stephane Clinchant, and Gabriela Csurka. Domain adaptation in the absence of source domain data. In *ACM SIGKDD International Conference on Knowledge Discovery and Data Mining*, 2016.
- [54] Xuhong Li, Yves Grandvalet, and Franck Davoine. Explicit inductive bias for transfer learning with convolutional networks. In *International Conference on Machine Learning*, 2018.
- [55] Xingjian Li, Haoyi Xiong, Hanchao Wang, Yuxuan Rao, Liping Liu, Zeyu Chen, and Jun Huan. Delta: Deep learning transfer using feature map with attention for convolutional networks. In *International Conference on Learning Representations*, 2019.
- [56] Kaichao You, Zhi Kou, Mingsheng Long, and Jianmin Wang. Co-tuning for transfer learning. *Advances in Neural Information Processing Systems*, 2020.
- [57] Yang Shu, Zhi Kou, Zhangjie Cao, Jianmin Wang, and Mingsheng Long. Zoo-tuning: Adaptive transfer from a zoo of models. In *International Conference on Machine Learning*, 2021.
- [58] Xinyang Chen, Sinan Wang, Bo Fu, Mingsheng Long, and Jianmin Wang. Catastrophic forgetting meets negative transfer: Batch spectral shrinkage for safe transfer learning. In *Advances in Neural Information Processing Systems*, 2019.
- [59] Takeru Miyato, Toshiki Kataoka, Masanori Koyama, and Yuichi Yoshida. Spectral normalization for generative adversarial networks. *International Conference on Learning Representations*, 2018.
- [60] Han Zhang, Ian Goodfellow, Dimitris Metaxas, and Augustus Odena. Self-attention generative adversarial networks. In *International conference on machine learning*, 2019.

- [61] Kang Minguk, Shim Woohyeon, Cho Minsu, and Park Jaesik. Rebooting acgan: Auxiliary classifier gans with stable training. In *Conference on Neural Information Processing Systems*, 2021.
- [62] Andre Martins and Ramon Astudillo. From softmax to sparsemax: A sparse model of attention and multi-label classification. In *International Conference on Machine Learning*, pages 1614–1623. PMLR, 2016.

Appendix

The following manuscript provides the supplementary materials of the main paper: Transfer Learning with Pre-trained Conditional Generative Models. We describe (A) additional related works of domain adaptation and fine-tuning, (B) details of experimental settings used in the main paper, (C) additional experiments including comparison of our method and fine-tuning, and detailed analysis of PP and P-SSL, and (D) qualitative evaluations of pseudo samples by PCS.

A Extended Related Work

A.1 Domain Adaptation

Domain adaptation leverages source knowledge to the target task by minimizing domain gaps between source and target domains through joint-training [3]. It is generally assumed that the source and target task label spaces overlap [1, 2] and labeled source datasets are available when training target models. Several studies have attempted to solve the transfer learning problems called source-free adaptation [53, 7, 8, 9], where the model must adapt to the target domain without target labels and the source dataset. However, they still require architecture consistency and overlaps between the source and target tasks, i.e., it is not applicable to our problem setting.

A.2 Finetuning

Our method is categorized as an inductive transfer learning approach [1], where the labeled target datasets are available and the source and target task label spaces do not overlap. In deep learning, fine-tuning [4, 40, 41], which leverages source pre-trained weights as initial parameters of the target models, is one of the most common approaches of inductive transfer learning because of its simplicity. Previous studies have attempted to improve fine-tuning by adding a penalty of the gaps between source and target models such as adding L^2 penalty term [54] or penalty using channel-wise importance of feature maps [55]. You et al. [56] have introduced category relationships between source and target tasks into target-task training and penalized the target models to predict pseudo source labels that are the outputs of the source models by applying target data. Shu et al. [57] have presented an approach leveraging multiple source models pre-trained on different datasets and tasks by mixing the outputs via adaptive aggregation modules. Although these methods outperform the naïve fine-tuning baselines, they require architecture consistency between source and target tasks. In contrast to the fine-tuning methods, our method can be used without architecture consistency and source dataset access since it transfers source knowledge via pseudo samples drawn from source pre-trained generative models.

B Details of Experiments

B.1 Knowledge Distillation Baselines

As stated in the main paper, we evaluated our method by comparing it with naïve knowledge distillation methods **Logit Matching** [28] and **Soft Target** [29]. We exploited Logit Matching and Soft Target for transfer learning under the architecture inconsistency since their loss functions use only final logit outputs of models regardless of the intermediate layers. To transfer knowledge in C_s to C_t , we first fine-tune the parameters of C_s on the target task then train C_t with knowledge distillation penalties by treating the trained C_s -based model as the teacher model. We optimized the knowledge distillation models by the following objective function:

$$\min_{\theta} \sum_{x_t, y_t \in \mathcal{D}_t} \mathcal{L}_{\text{sup}}(x_t, y_t, \theta) + \lambda_d \mathcal{L}_{\text{KD}}(l_{\theta}(x_t), l_{\phi}(x_t)), \quad (7)$$

where λ_d is a hyperparameter, \mathcal{L}_{KD} is a loss function of a knowledge distillation method, ϕ is the parameter of a teacher model, and $l_{\theta}(\cdot)$ and $l_{\phi}(\cdot)$ are the output of the logit function on θ and ϕ . In Logit Matching, \mathcal{L}_{KD} is a simple mean squared loss between l_{θ} and l_{ϕ} . Soft Target computes a Kullback-Leibler divergence between the softmax output of l_{θ} and the temperature softmax output of l_{ϕ} as \mathcal{L}_{KD} . We set the temperature parameter T to 4 by searching in $\{2, 4, 6\}$.

Table 10: Comparison of our methods with fine-tuning methods

	Top-1 Acc. (%)	
	Baseline	+ P-UDA
Pseudo Pre-training (Ours)	90.25 \pm 0.19	90.69 \pm 0.15
Fine-tuning	90.56 \pm 0.17	91.41 \pm 0.15
L2-SP [54]	91.20 \pm 0.05	91.43 \pm 0.10
DELTA [55]	91.52 \pm 0.26	91.66\pm0.29
BSS [58]	91.25 \pm 0.27	91.45 \pm 0.16
Co-Tuning [56]	91.08 \pm 0.15	91.16 \pm 0.05

Table 11: Performance comparison of multiple target architectures on StanfordCars (Top-1 Acc. (%))

	ResNet-50	WRN-50-2	MNASNet1.0	MobileNetV3-L	EfficientNet-B0	EfficientNet-B5
Scratch	76.21 \pm 1.40	76.92 \pm 2.16	81.08 \pm 0.06	82.67 \pm 0.21	82.50 \pm 0.47	85.09 \pm 1.01
Logit Matching	84.36 \pm 0.47	86.28 \pm 1.13	85.08 \pm 0.08	86.00 \pm 0.28	86.37 \pm 0.69	88.42 \pm 0.60
Soft Target	79.95 \pm 1.62	82.34 \pm 1.15	83.55 \pm 1.21	84.64 \pm 0.21	85.16 \pm 0.69	85.30 \pm 1.37
Pseudo Pre-training (PP)	90.25 \pm 0.19	90.95 \pm 0.21	87.14 \pm 0.05	88.19 \pm 0.14	88.27 \pm 0.33	89.50 \pm 0.17
P-UDA	80.14 \pm 0.57	78.90 \pm 0.82	82.22 \pm 0.16	83.26 \pm 0.21	83.22 \pm 0.54	85.82 \pm 0.47
PP + P-UDA	90.69\pm0.11	91.76\pm0.41	87.39\pm0.19	88.40\pm0.67	89.28\pm0.41	90.04\pm0.34
Fine-tuning (FT)	90.56 \pm 0.17	88.24 \pm 1.55	89.18 \pm 0.14	87.57 \pm 0.28	90.06 \pm 0.25	91.64 \pm 0.29
FT + P-UDA	91.41\pm0.15	91.95\pm0.09	89.46\pm0.15	88.19\pm0.15	90.13\pm0.14	91.71\pm0.09
R-UDA with ImageNet	77.48 \pm 0.46	77.93 \pm 1.45	81.74 \pm 2.19	82.17 \pm 0.75	82.25 \pm 1.03	83.86 \pm 1.54
FT + R-UDA	90.70 \pm 0.17	91.87 \pm 0.22	88.63 \pm 0.20	87.26 \pm 0.09	89.91 \pm 0.19	91.10 \pm 0.08

B.2 Filtering of Real Dataset by Relation to Target

We provide the details of the protocol of dataset filtering discussed in Sec. 3.4 of the main paper and list the correspondences between the target classes and selected source classes. For filtering datasets, we first calculated the confidence (the maximum probability of a class in the prediction) of the target samples by using the pre-trained source classifiers, then averaged the confidence scores for each target class, and finally selected the source classes with a confidence higher than 0.001 as the unlabeled dataset similar to [25]. We list the filtered ImageNet classes for each target dataset in Table 16 and 17.

B.3 Source Dataset: CompCars

CompCars [30] is a fine-grained vehicle image dataset for classifying the vehicle manufacturers or models. It contains 163 manufacturer classes, 1,716 model classes, and 136,726 images of entire vehicles collected from the web. As the source dataset for PP and P-SSL, we used 163 manufacturer classes for training classifiers and conditional generative models since the manufacturer classes do not overlap with the classes of the target dataset, i.e., StanfordCars.

C Additional Experiments

C.1 Comparison of Our Method with Fine-tuning Methods

For assessing the practicality of our method, we additionally compare our method with the fine-tuning methods that require architecture consistency, i.e., **Fine-tuning**: naively training C_t by using the pre-trained weights of C_s as the initial weights. **L2-SP** [54]: fine-tuning with the L^2 penalty term between the current training weights and the pre-trained source weights. **DELTA** [55]: fine-tuning with a penalty minimizing the gaps of channel-wise outputs of feature maps between source and target models. **BSS** [58]: fine-tuning with the penalty term enlarging eigenvalues of training features to avoid negative transfer. **Co-Tuning** [56]: fine-tuning on source and target task simultaneously by translating the target labels to the source labels. We implemented these methods on the basis of the open source repositories provided by the authors. All of hyperparameters used in L2-SP, DELTA, BSS, and Co-Tuning are those in the respective papers: β for L2-SP and DELTA was 0.01, η for BSS

Table 12: Performance comparison of ResNet-50 classifiers on multiple target datasets (Top-1 Acc. (%))

	Caltech-256-60	CUB-200-2011	DTD	FGVC-Aircraft	Indoor67	OxfordFlower	OxfordPets	StanfordCars	StanfordDogs
Scratch	51.03 \pm 1.10	52.98 \pm 1.14	42.58 \pm 2.57	72.02 \pm 4.16	49.70 \pm 1.67	68.57 \pm 1.79	63.31 \pm 1.20	76.21 \pm 1.40	57.46 \pm 1.70
Logit Matching	55.22 \pm 1.25	64.10 \pm 0.85	39.49 \pm 1.67	78.87 \pm 2.05	56.12 \pm 1.16	69.03 \pm 1.25	70.69 \pm 1.11	84.36 \pm 0.47	66.22 \pm 1.36
Soft Target	53.65 \pm 0.39	57.86 \pm 0.85	41.17 \pm 2.52	77.26 \pm 0.62	50.92 \pm 0.91	66.51 \pm 3.02	62.93 \pm 3.75	79.95 \pm 1.62	58.71 \pm 3.71
Pseudo Pre-training (PP)	68.69 \pm 0.08	75.73 \pm 0.33	55.53 \pm 1.07	86.02 \pm 0.40	65.60 \pm 0.62	93.80\pm0.61	86.57 \pm 0.37	90.25 \pm 0.19	72.80 \pm 0.15
P-UDA	53.12 \pm 0.99	54.81 \pm 0.26	38.71 \pm 3.11	72.59 \pm 0.05	50.60 \pm 1.86	69.41 \pm 2.41	64.51 \pm 0.48	80.14 \pm 0.57	60.66 \pm 1.36
PP + P-UDA	70.02\pm0.62	76.01\pm0.58	56.35\pm1.07	86.54\pm0.31	66.84\pm0.15	90.35 \pm 0.12	87.85\pm0.59	90.69\pm0.11	73.56\pm0.25
Fine-tuning (FT)	75.02 \pm 0.09	76.69 \pm 0.40	65.59\pm0.60	86.67 \pm 0.39	70.27 \pm 0.99	95.76 \pm 0.05	87.73 \pm 0.05	90.56 \pm 0.17	75.79 \pm 0.30
FT + P-UDA	75.93\pm0.44	80.46\pm0.16	62.48 \pm 0.97	87.32\pm1.15	71.00\pm0.35	96.59\pm0.37	91.48\pm0.32	91.41\pm0.15	78.53\pm0.28
R-UDA with ImageNet	52.22 \pm 1.12	55.54 \pm 1.23	41.84 \pm 3.64	75.36 \pm 0.80	52.13 \pm 1.98	68.55 \pm 1.68	66.34 \pm 1.07	77.48 \pm 0.46	59.93 \pm 1.25
FT + R-UDA	76.16 \pm 0.16	80.38 \pm 0.16	61.52 \pm 0.40	87.08 \pm 0.51	61.52 \pm 0.83	96.20 \pm 0.04	90.33 \pm 0.11	90.70 \pm 0.17	78.27 \pm 0.19

Table 13: Comparison of multiple source generative models (StanfordCars)

Source Generative Model	Top-1 Acc. (%)		
	PP	P-UDA	FID($\mathcal{D}_{s \leftarrow t}, \mathcal{D}_t$)
128 \times 128 resolution			
SNGAN [59]	87.07 \pm 0.26	72.75 \pm 2.60	108.31
SAGAN [60]	89.10 \pm 0.19	77.66 \pm 2.15	58.67
BigGAN [23]	89.97 \pm 0.27	77.54 \pm 1.45	27.17
256 \times 256 resolution			
BigGAN [23]	90.25 \pm 0.19	80.14\pm0.57	19.92
ADM-G [16]	90.23 \pm 1.06	79.44 \pm 0.47	18.72
512 \times 512 resolution			
BigGAN [23]	90.14 \pm 0.24	78.38 \pm 1.61	17.87

was 0.001, and λ for Co-Tuning was 2.3. We also tested the models by combining our methods and the fine-tuning methods. Table 11 and 12 list the extended results of the experiments on multiple architectures and target datasets in Secs. 3.2 and 3.3, respectively. Table 10 summarizes the results using the fine-tuning variants. The +P-UDA column indicates the results of the combination models of a fine-tuning method and P-UDA. We confirm that our method (pseudo pre-training + P-UDA) achieved competitive or superior results to the naïve fine-tuning. This means that our method can improve target models as well as fine-tuning without architectures consistency. We also observed that P-UDA can outperform fine-tuning baselines by being combined with them. These results indicate that our P-UDA can be applied even if the source and target architectures are consistent.

C.2 Source Generative Models

Table 13 lists the results with the architectures of multiple generative models. We tested our method by using pseudo samples generated from the generative models for multiple resolutions including SNGAN [59], SAGAN [60], and ADM-G [16]. We implemented these generative models on the basis of open source repositories including pytorch-pretrained-BigGAN⁴, Pytorch-StudioGAN⁵ by Kang et al. [61], and guided-diffusion⁶ by Dhariwal [16]; we used the pre-trained weights distributed by the repositories. We measured the top-1 test accuracy on the target task (StanfordCars) and Fréchet Inception Distance (FID, [36]). In Table 13, the generative models with better FID scores tended to achieve a higher top-1 accuracy score with PP and P-UDA. Regarding the resolution, the models of 256 \times 256, the generated samples of which are the nearest to the input size of C_t (224 \times 224), were the best. From these results, we recommend using generative models synthesizing high-fidelity samples at a resolution close to the target models when applying our method.

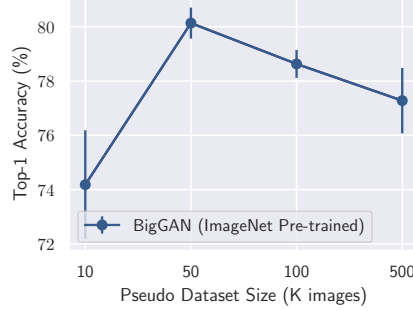


Figure 4: Top-1 accuracy of P-UDA when scaling pseudo dataset size

Table 14: Comparison of output label functions in PCS

	Top-1 Acc. (%)	FID
Random Label	75.55 ± 0.35	134.37
Softmax	80.14 ± 0.57	19.92
Temperature Softmax ($\tau = 0.4$)	80.04 ± 2.83	20.68
Argmax	78.89 ± 2.01	22.35
Sparsemax	76.08 ± 1.14	24.28
Classwise Mean	78.56 ± 2.83	22.14

C.3 Analysis of Pseudo Semi-supervised Learning

C.3.1 Sample Size

We evaluate the effect of the sizes of pseudo datasets for P-SSL on the target test accuracy. We varied the pseudo dataset sizes in $\{10K, 50K, 100K, 500K\}$ and tested the target performance of P-UDA on the StanfordCars dataset, as shown in Figure 4 (right). We found that the middle range of the dataset size (50K and 100K images) achieved better results. This suggests that P-SSL does not require generating extremely large pseudo datasets for boosting the target models.

C.3.2 Output Label Function

We discuss the performance comparison of output label functions in PCS. The output label function is crucial for synthesizing the target-related samples from source generative models since it directly determines the attributes on the pseudo samples. We tested six labeling strategies, i.e., **Random Label**: attaching uniformly sampled source labels, **Softmax**: using softmax outputs of C_s (default), **Temperature Softmax**: applying temperature scaling to output logits of C_s and using the softmax output, **Argmax**: using one-hot labels generated by selecting the class with the maximum probability in the softmax output of C_s , **Sparsemax** [62]: computing the Euclidean projections of the logit of C_t representing sparse distributions in the source label space, and **Classwise Mean**: computing the mean of softmax outputs of C_s for each target class and using it as representative pseudo source labels of the target class to generate pseudo samples. Table 14 shows the comparison of the labeling strategies. Among the strategies, Softmax is the best choice for PCS in terms of the target performance (top-1 accuracy) and the relatedness toward target datasets (FID). This means that the pseudo source label $y_{s \leftarrow t}$ by Softmax succeeds in representing the characteristics of a target sample x_t and its form of the soft label is important to extract target-related information via a source generative model G_s .

⁴<https://github.com/huggingface/pytorch-pretrained-BigGAN>

⁵<https://github.com/POSTECH-CVLab/PyTorch-StudioGAN>

⁶<https://github.com/openai/guided-diffusion>



Figure 5: Samples of source, target, and pseudo datasets (random picking).

Table 15: Ranking of averaged confidence scores of ImageNet classes corresponding to target classes

Rank	Target Class Label		
	All target classes	Hummer	Aston Martin V8 Convertible
1st	sports car (23.5%)	jeep (41.0%)	convertible (62.8%)
2nd	beach wagon (15.8%)	limousine (11.1%)	sports car (27.4%)
3rd	minivan (12.0%)	snowplow (6.7%)	racer (1.3%)
4th	convertible (10.0%)	moving van (6.7%)	pickup truck (1.3%)
5th	pickup truck (7.0%)	tow truck (6.3%)	car wheel (1.3%)

D Qualitative Evaluation of Pseudo Samples

We discuss qualitative studies of the pseudo samples generated by PCS. To confirm the correspondences between the target and pseudo samples, we used StanfordCars as the target dataset and generated samples from BigGAN with the same setting as in Sec. 3. Figure 5 shows the visualizations of the source dataset (ImageNet), target dataset (StanfordCars), and pseudo samples generated by PCS. The samples were randomly selected from each dataset. We can see that PCS succeeded in generating target-related samples from the target samples. To assess the validity of using pseudo source soft labels in PCS, we analyzed the pseudo samples corresponding to each target label. Figure 6 shows the pseudo samples generated by the target samples of Hummer and Aston Martin V8 Convertible classes in StanfordCars. We confirm that the pseudo samples by PCS can capture the features of target classes. This also can confirm the ranking of the confidence scores for source classes listed in Table 15; the pseudo source soft labels seem to represent the target samples by the interpolation of source classes.

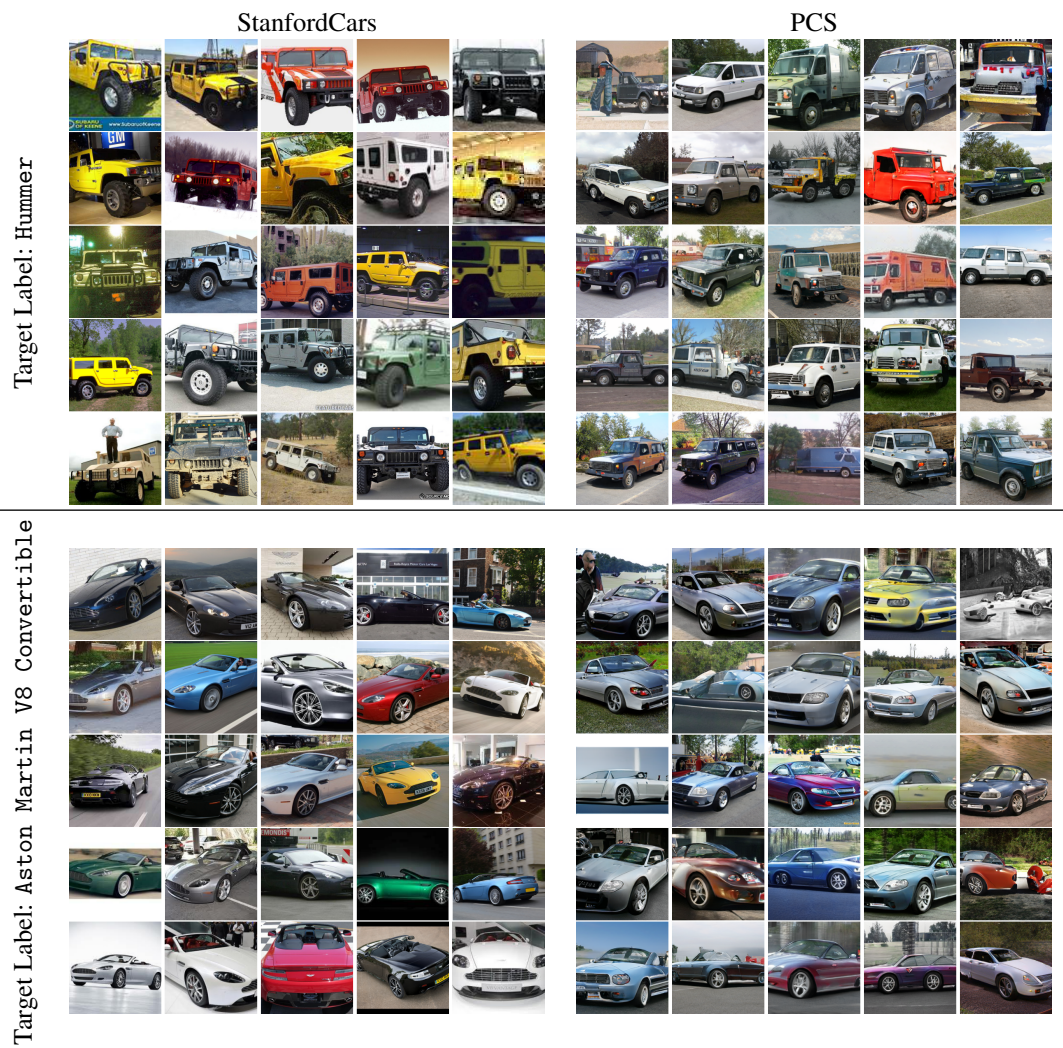


Figure 6: Pseudo samples generated by PCS (random picking)

Table 16: Corresponding ImageNet classes to target datasets (1)

Target Dataset	ImageNet Classes
Caltech-256-60	goldfish, electric ray, ostrich, great grey owl, tree frog, tailed frog, loggerhead, leatherback turtle, common iguana, triceratops, trilobite, scorpion, barn spider, tick, centipede, hummingbird, drake, goose, tusker, wallaby, jellyfish, nematode, conch, snail, rock crab, fiddler crab, American lobster, isopod, black stork, American egret, king penguin, killer whale, whippet, Saluki, leopard, jaguar, cheetah, brown bear, American black bear, fly, grasshopper, cockroach, mantis, monarch, starfish, sea urchin, porcupine, sorrel, zebra, ibex, hartebeest, Arabian camel, llama, skunk, gorilla, chimpanzee, Indian elephant, African elephant, acoustic guitar, airliner, airship, altar, analog clock, assault rifle, backpack, balloon, ballpoint, Band Aid, barbell, barrow, bathtub, beacon, beaker, bearskin, beer glass, bell cote, bicycle-built-for-two, binder, binoculars, bolo tie, bottlecap, bow, brass, breastplate, buckle, candle, cannon, canoe, can opener, carpenter's kit, car wheel, cassette, cassette player, CD player, chain, chest, chime, clog, coffee mug, coffeepot, coil, combination lock, corkscrew, cowboy hat, cradle, crane, crash helmet, croquet ball, desktop computer, dial telephone, doormat, drilling platform, drum, dumbbell, electric fan, electric guitar, envelope, face powder, fire engine, fire screen, flagpole, folding chair, football helmet, fountain, French horn, frying pan, gasmask, gas pump, goblet, golf ball, gong, grand piano, guillotine, hair slide, hamper, hand blower, hand-held computer, handkerchief, harmonica, harp, harvester, hook, horse cart, hourglass, iPod, jersey, jigsaw puzzle, joystick, knee pad, ladle, lampshade, laptop, lawn mower, letter opener, lighter, loudspeaker, loupe, lumbermill, magnetic compass, mailbag, mailbox, maraca, marimba, maze, microphone, microwave, missile, modem, moped, mortar, mosque, mountain bike, mountain tent, mouse, mousetrap, muzzle, nail, neck brace, nipple, notebook, obelisk, ocarina, oil filter, oscilloscope, oxygen mask, packet, paddle, palace, parachute, park bench, pay-phone, pedestal, pencil sharpener, perfume, Petri dish, photocopier, pick, pier, pill bottle, ping-pong ball, pitcher, plane, pole, pool table, pot, printer, projectile, projector, puck, punching bag, quill, racket, radio, radio telescope, reel, refrigerator, revolver, rifle, rubber eraser, rule, running shoe, safety pin, sandal, scabbard, scale, school bus, schooner, screen, screw, screwdriver, shield, ski, slot, snowmobile, soap dispenser, soccer ball, sock, solar dish, sombrero, space bar, spatula, speedboat, spotlight, stethoscope, stopwatch, stretcher, studio couch, sunglass, sunscreen, suspension bridge, swing, switch, syringe, table lamp, tape player, teapot, teddy, tennis ball, thimble, thresher, toaster, tobacco shop, toilet seat, torch, tow truck, tray, tricycle, tripod, tub, typewriter keyboard, umbrella, unicycle, upright, vase, waffle iron, wall clock, wallet, warplane, washer, water jug, whiskey jug, whistle, Windsor tie, wine bottle, wool, worm fence, yawl, web site, comic book, street sign, traffic light, book jacket, plate, cheeseburger, hotdog, spaghetti squash, fig, carbonara, red wine, cup, eggnog, cliff, geyser, lakeside, promontory, seashore, valley, volcano, daisy, hip, earthstar, hen-of-the-woods
CUB-200-2011	hen, brambling, goldfinch, house finch, junco, indigo bunting, robin, bulbul, jay, magpie, chickadee, water ouzel, kite, bald eagle, vulture, great grey owl, black grouse, ptarmigan, ruffed grouse, prairie chicken, quail, partridge, macaw, lorikeet, coucal, bee eater, hornbill, hummingbird, jacamar, toucan, drake, red-breasted merganser, goose, black swan, white stork, black stork, spoonbill, little blue heron, American egret, bittern, crane, limpkin, European gallinule, American coot, bustard, ruddy turnstone, red-backed sandpiper, redshank, dowitcher, oystercatcher, pelican, king penguin, albatross, worm fence
DTD	electric ray, stingray, leatherback turtle, thunder snake, hognose snake, horned viper, sidewinder, trilobite, harvestman, barn spider, black widow tick, jellyfish, sea anemone, brain coral, flatworm, nematode, conch, sea slug, chiton, chambered nautilus, fiddler crab, isopod, komondor, tiger, leaf beetle, dung beetle, bee, ant, walking stick, cockroach, sea urchin, sea cucumber, zebra, apron, backpack, bakery, balloon, Band Aid, bannister, bath towel, beer glass, bib, binder, bonnet, bottlecap, bow tie, breastplate, broom, buckle, candle, cardigan, chain, chainlink fence, chain mail, cliff dwelling, cloak, coil, confectionery, crate, cuirass, dishrag, dome, doormat, envelope, face powder, feather boa, fire screen, fountain, fur coat, golf ball, gown, hair slide, hamper, handkerchief, honeycomb, hook, hoopskirt, jean, jersey, jigsaw puzzle, knot, lampshade, lighter, loudspeaker, mailbag, manhole cover, mask, matchstick, maze, megalith, microphone, mitten, mosquito net, nail, necklace, overskirt, packet, padlock, paintbrush, pajama, paper towel, pencil box, Petri dish, picket fence, pillow, pinwheel, plastic bag, poncho, pot, prayer rug, prison, purse, quill, quilt, radiator, radio, rubber eraser, rule, safety pin, saltshaker, sarong, screw, shield, shoji, shopping basket, shovel, shower cap, shower curtain, sleeping bag, solar dish, space heater, spider web, stole, stone wall, strainer, swab, sweatshirt, swimming trunks, switch, syringe, tennis ball, thatch, theater curtain, thimble, tile roof, tray, trench coat, umbrella, vase, vault, velvet, waffle iron, wall clock, wallet, wardrobe, water bottle, wig, window screen, window shade, Windsor tie, wooden spoon, wool, web site, crossword puzzle, book jacket, trifle, ice cream, ice lolly, French loaf, pretzel, head cabbage, broccoli, cauliflower, strawberry, lemon, fig, jackfruit, custard apple, pomegranate, hay, chocolate sauce, dough, meat loaf, potpie, cup, eggnog, bubble, cliff, coral reef, geyser, sandbar, valley, volcano, corn, buckeye, coral fungus, hen-of-the-woods, ear, toilet tissue
FGVC-Aircraft	aircraft carrier, airliner, airship, missile, projectile, space shuttle, speedboat, trimaran, warplane, wing
Indoor67	academic gown, altar, bakery, balance beam, bannister, barbell, barber chair, barbershop, barrel, bathing cap, bathtub, beer bottle, bookcase, bookshop, bullet train, butcher shop, carousel, carton, cash machine, china cabinet, church, cinema, coil, confectionery, cradle, crate, crib, crutch, desk, desktop computer, dining table, dishwasher, dome, drum, dumbbell, electric locomotive, entertainment center, file, fire screen, folding chair, forklift, fountain, four-poster, golfcart, grand piano, greenhouse, grocery store, guillotine, home theater, horizontal bar, jigsaw puzzle, lab coat, laptop, library, limousine, loudspeaker, lumbermill, marimba, maze, medicine chest, microwave, minibus, monastery, monitor, mosquito net, organ, oxygen mask, palace, parallel bars, passenger car, patio, photocopier, pier, ping-pong ball, planetarium, plate rack, pole, pool table, pot, potter's wheel, prayer rug, printer, prison, projector, quilt, radio, refrigerator, restaurant, rocking chair, rotisserie, scoreboard, screen, shoe shop, shoji, shopping basket, shower curtain, sliding door, slot, solar dish, spotlight, stage, steel arch bridge, stove, streetcar, stretcher, studio couch, table lamp, tape player, television, theater curtain, throne, tobacco shop, toilet seat, toyshop, tripod, tub, turnstile, upright, vacuum, vault, vending machine, vestment, wardrobe, washbasin, washer, window screen, window shade, wine bottle, wok, comic book, plate, groom

Table 17: Corresponding ImageNet classes to target datasets (2)

Target Dataset	ImageNet Classes
OxfordFlower	goldfish, cock, harvestman, garden spider, hummingbird, sea anemone, conch, snail, slug, sea slug, chambered nautilus, ladybug, long-horned beetle, leaf beetle, fly, bee, ant, grasshopper, cricket, walking stick, mantis, lacewing, admiral, ringlet, monarch, cabbage butterfly, sulphur butterfly, lycaenid, sea urchin, birdhouse, bonnet, candle, chainlink fence, greenhouse, hair slide, hamper, handkerchief, lotion, paper towel, perfume, picket fence, pinwheel, plastic bag, pot, quill, shower cap, tray, umbrella, vase, velvet, wool, head cabbage, cauliflower, zucchini, spaghetti squash, acorn squash, butternut squash, cucumber, artichoke, bell pepper, cardoon, mushroom, strawberry, orange, lemon, fig, pineapple, custard apple, pomegranate, coral reef, rapeseed, daisy, yellow lady's slipper, corn, acorn, hip, buckeye, coral fungus, stinkhorn, earthstar, hen-of-the-woods, ear
OxfordPets	Chihuahua, Japanese spaniel, Maltese dog, Pekinese, Shih-Tzu, Blenheim spaniel, papillon, toy terrier, Rhodesian ridgeback, basset, beagle, bloodhound, bluetick, Walker hound, English foxhound, redbone, Italian greyhound, Ibizan hound, Norwegian elkhound, Weimaraner, Staffordshire bullterrier, American Staffordshire terrier, Irish terrier, Norwich terrier, Yorkshire terrier, Lakeland terrier, cairn, Australian terrier, Dandie Dinmont, Boston bull, Scotch terrier, Tibetan terrier, silky terrier, soft-coated wheaten terrier, West Highland white terrier, Lhasa, flat-coated retriever, golden retriever, Labrador retriever, Chesapeake Bay retriever, German short-haired pointer, English setter, Brittany spaniel, English springer, Welsh springer spaniel, cocker spaniel, kuvasz, schipperke, groenendael, kelpie, German shepherd, miniature pinscher, boxer, bull mastiff, Tibetan mastiff, French bulldog, Great Dane, Saint Bernard, Eskimo dog, Siberian husky, affenpinscher, basenji, pug, Leonberg, Newfoundland, Great Pyrenees, Samoyed, Pomeranian, chow, keeshond, Brabancon griffon, Pembroke, toy poodle, miniature poodle, Mexican hairless, white wolf, dingo, tabby, tiger cat, Persian cat, Siamese cat, Egyptian cat, lynx, bath towel, bucket, carton, plastic bag, quilt, sleeping bag, space heater, tennis ball, window screen
StanfordCars	ambulance, amphibian, beach wagon, cab, car wheel, convertible, grille, jeep, minibus, limousine, minivan, mobile home, moving van, parking meter, passenger car, pickup, police van, racer, recreational vehicle, snowplow, sports car, tow truck, trailer truck
StanfordDogs	Chihuahua, Japanese spaniel, Maltese dog, Pekinese, Shih-Tzu, Blenheim spaniel, papillon, toy terrier, Rhodesian ridgeback, Afghan hound, basset, beagle, bloodhound, bluetick, black-and-tan coonhound, Walker hound, English foxhound, redbone, borzoi, Irish wolfhound, Italian greyhound, whippet, Ibizan hound, Norwegian elkhound, otterhound, Saluki, Scottish deerhound, Weimaraner, Staffordshire bullterrier, American Staffordshire terrier, Bedlington terrier, Border terrier, Kerry blue terrier, Irish terrier, Norfolk terrier, Norwich terrier, Yorkshire terrier, wire-haired fox terrier, Lakeland terrier, Sealyham terrier, Airedale, cairn, Australian terrier, Dandie Dinmont, Boston bull, miniature schnauzer, giant schnauzer, standard schnauzer, Scotch terrier, Tibetan terrier, silky terrier, soft-coated wheaten terrier, West Highland white terrier, Lhasa, flat-coated retriever, curly-coated retriever, golden retriever, Labrador retriever, Chesapeake Bay retriever, German short-haired pointer, vizsla, English setter, Irish setter, Gordon setter, Brittany spaniel, clumber, English springer, Welsh springer spaniel, cocker spaniel, Sussex spaniel, Irish water spaniel, kuvasz, schipperke, groenendael, malinois, briard, kelpie, komondor, Old English sheepdog, Shetland sheepdog, collie, Border collie, Bouvier des Flandres, Rottweiler, German shepherd, Doberman, miniature pinscher, Greater Swiss Mountain dog, Bernese mountain dog, Appenzeller, Entlebucher, boxer, bull mastiff, Tibetan mastiff, French bulldog, Great Dane, Saint Bernard, Eskimo dog, malamute, Siberian husky, affenpinscher, basenji, pug, Leonberg, Newfoundland, Great Pyrenees, Samoyed, Pomeranian, chow, keeshond, Brabancon griffon, Pembroke, Cardigan, toy poodle, miniature poodle, standard poodle, Mexican hairless, dingo, dhole, African hunting dog